NASA TECHNICAL NOTE

NASA TN D-7219

NASA TN D-7219

HEAT PIPE INVESTIGATIONS

by James P. Marshburn

Goddard Space Flight Center

Greenbelt, Md. 20771

NATIONAL AERONAUTICS AND SPACE ADMINISTRATION • WASHINGTON, D. C. • AUGUST 1973

1. Report No.	2. Government Accession No.	3. Recipient's Catalog No.
NASA TN D-7219		

4. Title and Subtitle	5. Report Date
Heat Pipe Investigations	August 1973
	6. Performing Organization Code: 322
7. Author(s): James P. Marshburn	8. Performing Organization Report No.: G-7311
9. Performing Organization Name and Address: Goddard Space Flight Center, Greenbelt, Maryland 20771	10. Work Unit No.: 831-41-25-02
	11. Contract or Grant No.
	13. Type of Report and Period Covered: Technical Note
12. Sponsoring Agency Name and Address: National Aeronautics and Space Administration, Washington, D. C. 20546	14. Sponsoring Agency Code

15. Supplementary Notes

16. Abstract

Heat pipes are being used in many engineering applications today and promise to play an ever-increasing role in future heat transfer processes. Techniques associated with thermal-vacuum and bench testing, along with flight testing of the OAO-C spacecraft heat pipes are outlined, to show that the processes used in heat transfer design and testing are adequate for good performance evaluations.

17. Key Words (Selected by Author(s))	18. Distribution Statement
Heat Pipe Performance, Analytic Equations, Fluid Selection, Material Capability	Unclassified—Unlimited

19. Security Classif. (of this report)	20. Security Classif. (of this page)	21. No. of Pages	22. Price*
Unclassified	Unclassified	44	$3.00

* For sale by the National Technical Information Service, Springfield, Virginia 22151

SUMMARY

The heat pipe is becoming one of the most valuable tools of the heat transfer engineer. This document presents an introduction to the basic characteristics of heat pipes, their method of functioning, the analytical equations used to gage the heat transfer capabilities, and the results obtained from the thermal vacuum, bench, and flight tests of the heat pipes for the Orbiting Astronomical Observatory spacecraft.

The sections on the selection of fluids, pipe materials, and wick materials indicate the logic used in the design of the heat pipes. The test results indicate the value of research and of performance predictions, and demonstrate the actual performance of the pipes. The test results are sufficiently accurate to prove the value of heat pipes for use in spacecraft as well as in equipment used on the ground.

CONTENTS

CONTENTS – (continued)

HEAT PIPE INVESTIGATIONS

James P. Marshburn
Goddard Space Flight Center

INTRODUCTION

The intent of this document is to introduce the novice to some heat pipe manufacturing problems, modes of operation, bench and thermal-vacuum test problems, and some zero-G flight data for ground comparisons. A heat pipe is basically a superconductor that tends to transfer heat by vapor and liquid transport at near isothermal conditions. This operational principle was first described by Gaugler as cited by Eastman in 1942, but was overlooked until 1963, when Grover investigated the principles and the possible space applications in detail.

The basic mode of operation for a heat pipe occurs when fluid in a thin-walled container is subjected to heating over some external area and passive or active cooling occurs over some or all of the remaining area. Since the fluid is in a two-phase state, evaporation and condensation occur in the hot and cold regions of the pipe respectively. Thus, heat is transported as a function of the latent heat of vaporization property and the liquid or vapor mass flow rate.

Although heat pipes have been employed in recently launched satellites, such as the Applications Technology Satellite-E (1969), Package Attitude Control (1969), Orbiting Astronomical Observatory-B (OAO-B, 1970), and in OAO-C (launched in August, 1972), questions such as to how to test the heat pipe units on the ground and how to extrapolate the results to the zero-gravity flight conditions have not been completely resolved. To aid in the understanding of this problem, a series of bench and thermal-vacuum tests were conducted and compared to flight data taken from the OAO-C spacecraft. The results of this series of tests and the final analysis are given in the test results section. Prior to this, a brief discussion of some of the design and functional problems of typical heat pipes is presented.

HEAT PIPE DESIGN

The heat pipe is basically a thin-walled tube which contains a heat-transporting fluid and a wick or wicking device to provide for movement of the liquid by capillary attraction. As used in the Orbiting Astronomical Observatory, and illustrated in Figure 1, each of three heat pipes is a tube of 1.27 cm (one-half in.) diameter with closed ends, bent in the form of a torus of 1.19 m (46.9 in.) diameter). These heat pipes are placed in the annulus formed by the central experiment tube and the spacecraft structural cavity, and surround an experimental telescope; they aid in keeping local sections of the instrument at approximately the same temperature, within ±3° C, and help to maintain the isothermalization of the entire spacecraft.

In the basic design of a heat pipe, the first consideration is choice of the fluid which will be used, in order to operate within a specified thermal range. Then the tube or container and the type of wicking device can be designed. The three elements are closely related and the tube and wick must match the requirements of the fluid.

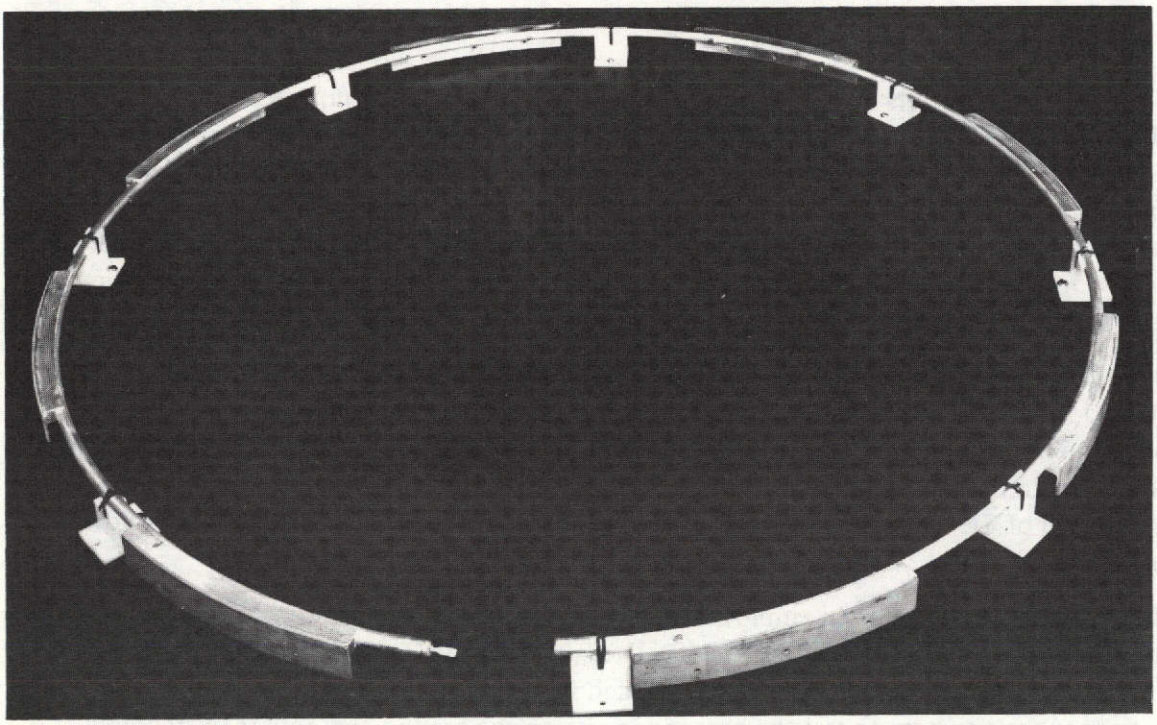

Figure 1. Heat pipe used in the Orbiting Astronomical Observatory.

Choice of Fluid

The basic choice of a working fluid depends upon many factors, but for OAO-C and for most near-Earth satellites and deep-space probes the required thermal operating limits constitute the most critical parameter. These limits are in general −80° C to +60° C. Other factors which must be considered in the selection of the working fluid are:

- Compatibility with other materials in the pipe and spacecraft
- High latent heat of vaporization
- Low vapor pressure
- Wettability
- Low liquid viscosity

Compatibility

For prolonged operating lifetime the working fluid must be chemically compatible with its wick and container, and sometimes with the spacecraft. In the case of the OAO-B heat pipes, an additional restriction was placed upon the choice of fluid, in that the fluid had to be compatible with the optical systems on the spacecraft. This requirement was made to ensure the safety of the optical systems in the event that a meteoroid were to puncture a heat pipe, which would cause the fluid to come into contact with the internal and external systems on the spacecraft. Based on this consideration, one of the freons was selected for the OAO-B heat pipes. This fluid also provided a low internal vapor pressure, which in turn permitted minimum wall thickness and minimum weight. Anhydrous ammonia was selected for the later OAO-C heat pipes, because ammonia can carry more heat than the freons, and allows the heat pipe to function better.

Latent Heat of Vaporization

Latent heat of vaporization, h_{fg}, is the additional quantity of heat required to convert a liquid to a gas once the liquid has reached its boiling temperature. The value, on a per gas basis, is a function of pressure and temperature. The desirability of having a high h_{fg} is directly related to the maximum heat which can be transferred by a heat pipe. This is due to the fact that the heat transfer limit of any heat pipe is equal to the product of its mass flow rate and the latent heat of vaporization of the liquid used.

Vapor Pressure

Because of safety factors, low vapor pressure is desirable, since the tube wall thickness is directly related to the internal pressure. One of the heat pipes for the Applications Technology Satellite-F exploded during its qualification testing, due to a combination of high internal vapor pressure and extreme wall thinness. Since that pipe was known to be thin, as determined by ultrasonic measurements, the proper precautions had been taken and the explosion caused no damage. However, the result of that test points out the necessity of having a high factor of safety which can be partially achieved by having a low vapor pressure.

Wettability

In order for a heat pipe to function properly, reducing the hot spots or thermal gradients, the liquid must thoroughly wet the wick and the containing vessel. This wetting ability (which is hard to measure) is directly proportional to the cosine of the wetting angle. Figures 2 and 3 indicate a static arrangement for determining the wetting angle, θ, and the capillary pull, ΔP. When $\theta = 0$ degree, the pipe is said to be completely wet; and when $\theta =$ 90 degrees or greater, the pipe is dry. It is virtually impossible to determine this parameter in a flowing system. For this reason heat pipe designers usually calculate how much fluid is required to completely soak the heat pipe internal structural walls and wick, and load the pipe at a prescribed temperature with this amount of fluid, plus or minus 5 to 10 percent.

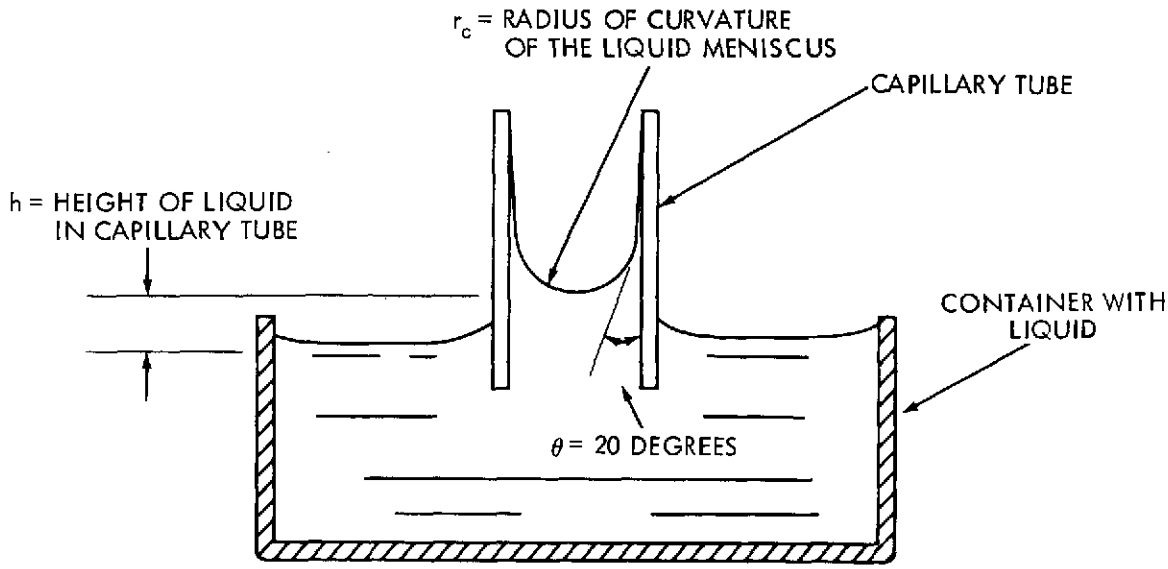

Figure 2. Capillary attraction (rise of liquid in capillary tube) and wetting angle.

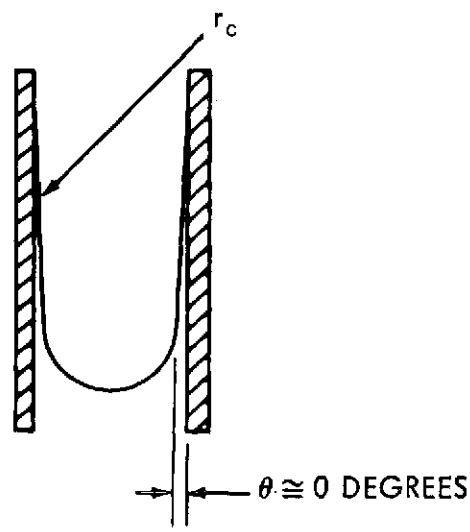

Figure 3. Complete wetting of tube when wetting angle $\theta = 0$ degree.

For the static arrangement shown in Figure 2, the capillary pull, ΔP_c, is defined as the limit where the weight of the fluid column equals the gravitational force, or $\Delta P_c = \rho gh$ for this case. The height of the liquid in the capillary tube, h, is a variable, and can be raised or lowered depending upon the design of the wicking structure. Because most fluids entering the tube will form a concave surface, extending farther up the sides of the tube than at the center, as in a glass of water, the tube can be dry only when $\theta = 90$ degrees or greater.

Complete wettability, $\theta \cong 0$ degree, as shown in Figure 3 is more difficult to visualize. As the radius of curvature (r_c) shrinks, the fluid must extend higher up the walls of the tube until a limiting case is reached, where r_c equals approximately one-half the tube diameter. In this case the fluid assumes a profile parallel to the sides of the tube, which yields the limit of $\theta \cong 0$ degree. Theory predicts that this occurs most readily in low and zero-G environments, and this is proven by free-fall experiments. Among the various fluids which can be used, mercury is a notable exception in that it does not extend up the tube and does not wet the tube. The reason for this is that it has high surface tension.

Surface tension forces allow liquids in free fall to form spheroidal shapes. This occurs because surface tension forces tend to form minimum surface areas for all fluids. In general this minimum-surface ability increases for all fluids as the temperature drops below ambient; i.e., the surface-tension forces increase for all fluids, but vary in strength depending upon the fluid used. In a thermal-vacuum test of one of the anhydrous-ammonia-charged pipes for the OAO-C spacecraft, it was shown in a low temperature test at −45° C that high values of surface tension or overfill caused the liquid to collect in the condenser sections (the cold sections of the heat pipe), which created an out-of-tolerance condition in reference to the test specification. Further tests indicated that anhydrous ammonia can be used successfully in the −40° to + 50° C temperature range when the proper materials are used for tube and wicking structure.

Viscosity

Low liquid viscosity allows the fluid to flow more freely in the return-flow portions of the pipe, producing less drag; and this in turn provides better heat transport, preventing high temperature gradients along the length of the pipe.

Liquid Transport Factor

A standard way of analyzing the capacity of a liquid to transport heat is based upon a lumped parameter of all the fluid properties. This is sometimes called a figure of merit, but more recently it is referred to as the liquid transport factor, N_f. This is given as

$$N_f = \frac{\sigma \rho_f h_{fg}}{\mu f}$$

where

σ = fluid surface tension

ρ_f = fluid density

h_{fg} = latent heat of vaporization

μ_f = fluid viscosity

A graph of the liquid transport factor, covering a wide thermal band, is given in Figure 4 for various working fluids. This graph indicates the temperature range in which each fluid can be used. However, for the use of any given fluid, experience dictates that a careful analysis of each property embodied in N_f is warranted. For example, a high value of latent heat of vaporization, high fluid density, and high fluid surface tension would usually be desirable, in conjunction with low viscosity. However, if the fluid density is sufficiently high, the force required to pump the fluid may not be great enough and may inhibit the flow of the fluid, resulting in unsatisfactory thermal gradients. Therefore, in choosing any heat pipe fluid, almost all conceivable parameters must be considered.

Choice of Container Material

Once the fluid has been selected for a given thermal range, the design of the external container and the selection of the material can be finalized. The criteria which must be considered in selecting the container material are as follows:

- The fluid and container compatibility
- The maximum power density to be absorbed by the pipe
- The external and internal forces acting on the container

Material

Because the container and the fluid must be chemically compatible, the choice is usually limited to a few pipe materials for any given fluid. The materials which have been used thus far include aluminum, copper, stainless steel, and glass, all of which were tested at Goddard; and nickel, ceramic, and alloys of molybdenum, tantalum, and niobium, which were tested in private industry.

Aluminum 6061-T6, in the form of a seamless tube, has been the most commonly used material because of its low weight, ease of machining, and its compatibility with many fluids. Aluminum has been used on heat pipes for the OAO-B, OAO-C, ATS-E, and ATS-F spacecraft.

Other factors involved in the selection of the container material are the machining and heating processes that the item must undergo after it has been charged or filled with its working fluid. These include the types of mechanical support, whether the pipe is bonded

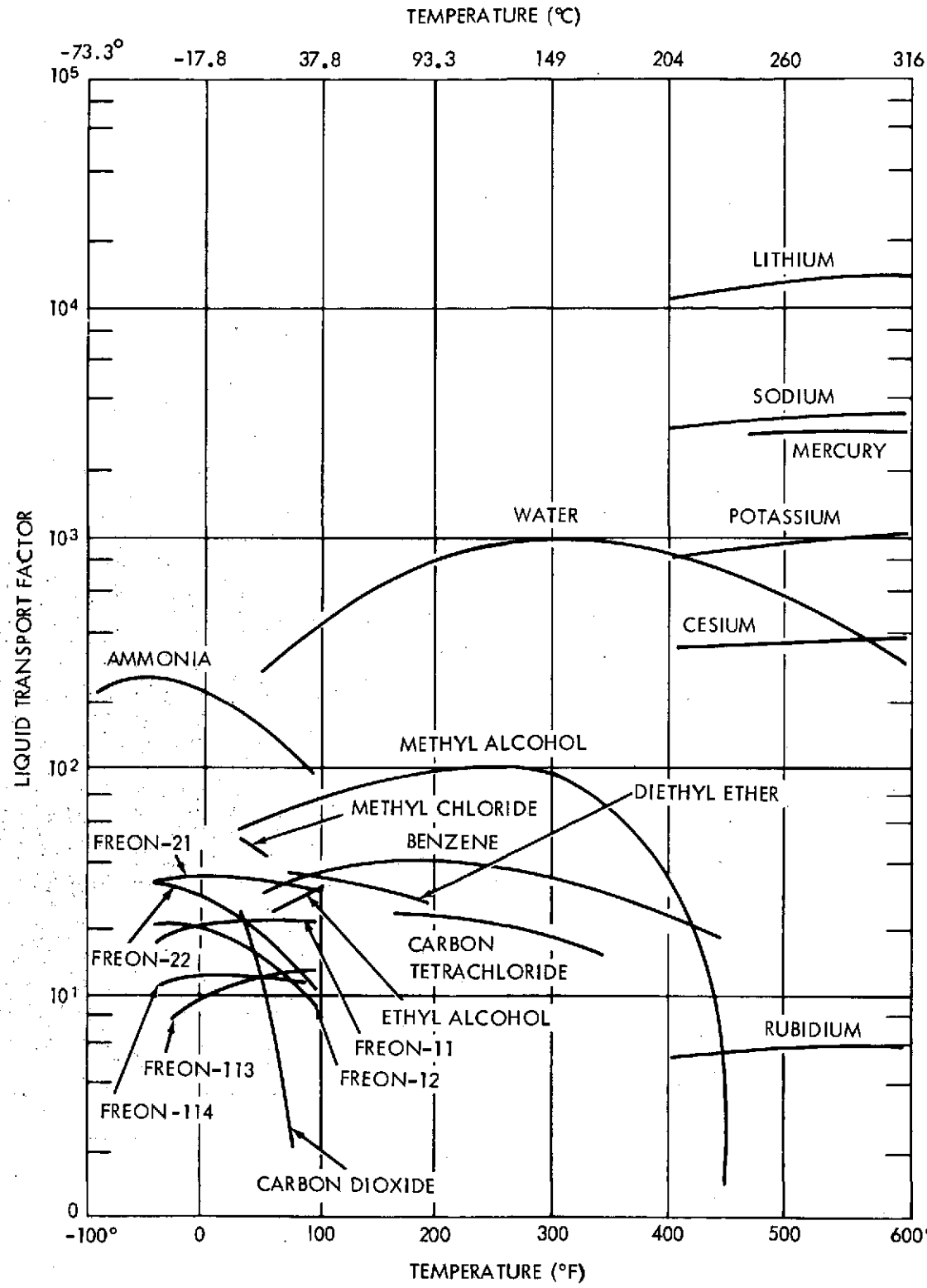

Figure 4. Liquid transport factor (figure of merit) for various liquids.

or welded in place, and other processes which must be endured while the pipe is being assembled into its final working location.

The problem of processing the tube after filling caused great concern for the ATS-F spacecraft heat pipes, when a high temperature process became necessary before some of the heat pipes could be completely encased in honeycomb panels which formed the spacecraft walls and support decks. The problems associated with such processes could require alterations to the diameter and wall thickness of the pipe and to its manufacturing process.

Power Density

The maximum allowable power density, i.e., the maximum heat input into a pipe, is a function of four variables: the input area, the wicking device, the working fluid, and the thermal gradient required by the spacecraft.

Power density is specified as watts per unit area, and this is different from total power, since total power can be applied over a large or small area. Thus any given heat pipe system can take only a certain concentration of power before the capillary pumping limit of the wick is overtaxed, and dryout—or burnout—occurs. It is likely that the required thermal gradient limit of any spacecraft which uses heat pipes could be exceeded long before burnout occurs.

The limitation posed by the working fluid is strictly a function of the ability of that fluid's figure of merit. Thus, much depends upon the fluid which is used; the liquid with the highest h_{fg} will yield a lower thermal gradient for the same power density.

External and Internal Forces

External and internal forces are of prime importance to the proper functioning of the pipe. One of the ammonia filled pipes for OAO-C had an internal pressure of approximately 200 psig at 20° C. At 54° C, the vapor pressure was 760 psig. This would have presented a serious health problem to nearby personnel if the pipe had accidentally ruptured or if it had been dropped during testing. The external forces which must be considered are those created by acceleration during launch and by spinning or tumbling in orbit. The pipe must be strong enough to withstand all these forces in combination. Heat pipes with internal pressures of 0.03 to 10 atmospheres have been operated successfully in laboratories for periods of up to 8 years.

Choice of Wicking Device

In addition to the working fluid and the container, the third essential part of the heat pipe is the wicking device (capillary or wicking structure), which facilitates the movement of the cool liquid to the warm or hot evaporator section of the pipe. As shown by the numerous cross sections of heat pipes in Figure 5, the only limit on the basic design of the wicking structure is the experience and imagination of the designer.

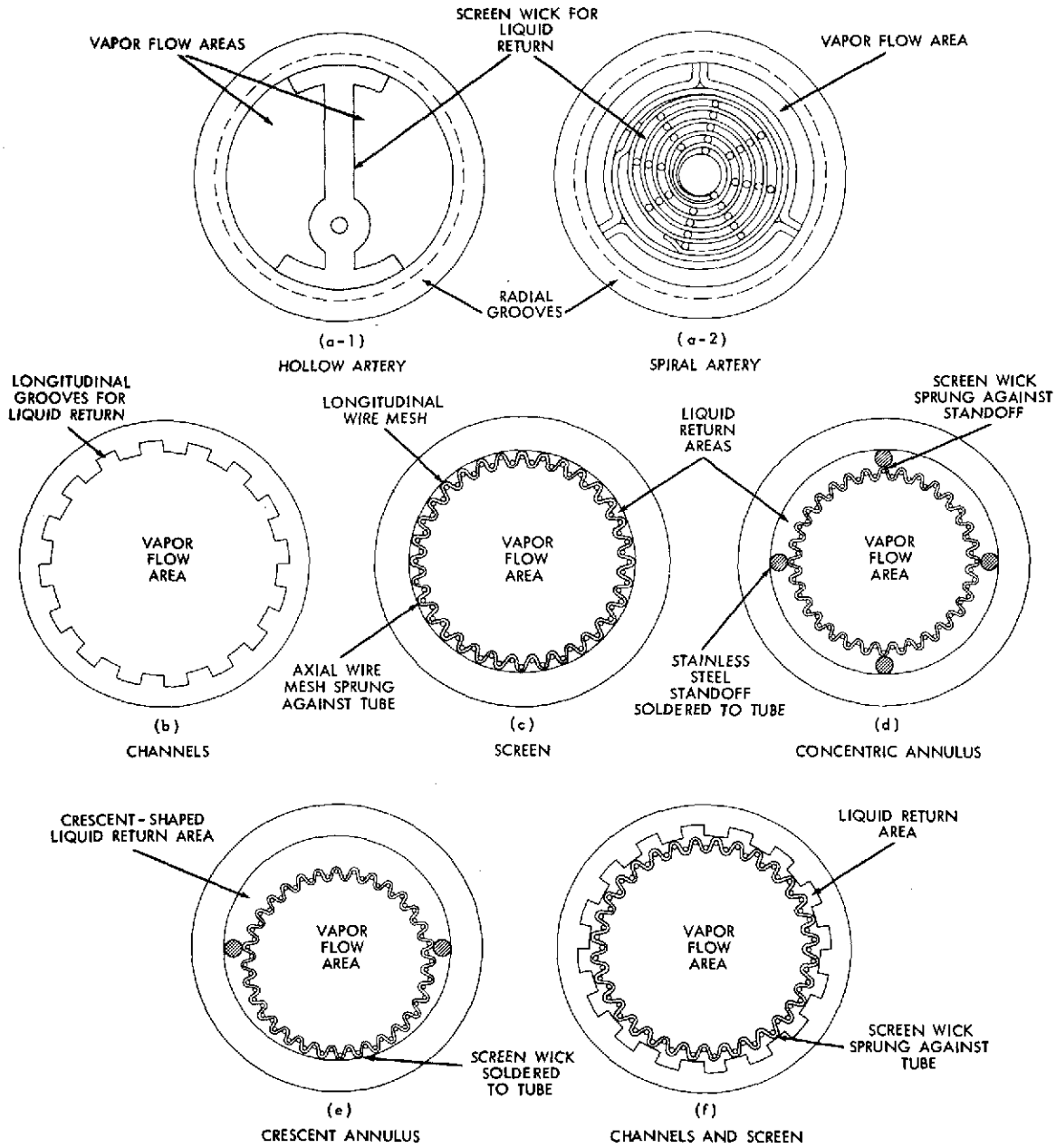

Figure 5. Cross sections of various types of wicking devices.

The wicking structure is similar to and performs the same function as the wick in a kerosene lamp: It provides a fine mesh capillary structure which moves the liquid from one point to another, in both cases from a point of high liquid pressure and cooler temperature to a point or points of lower liquid pressure and higher temperature.

The wicking device shown in detail in Figure 6 consists of a section of 304 stainless steel screen, 100 mesh per 2.54 cm (1 in.), which is 90.2 cm (35.50 in.) wide and approximately 10.2 cm (400 in.) long. This screen is welded along one long edge to a 310 stainless steel wire core 1.6 mm (0.063 in.) in diameter.

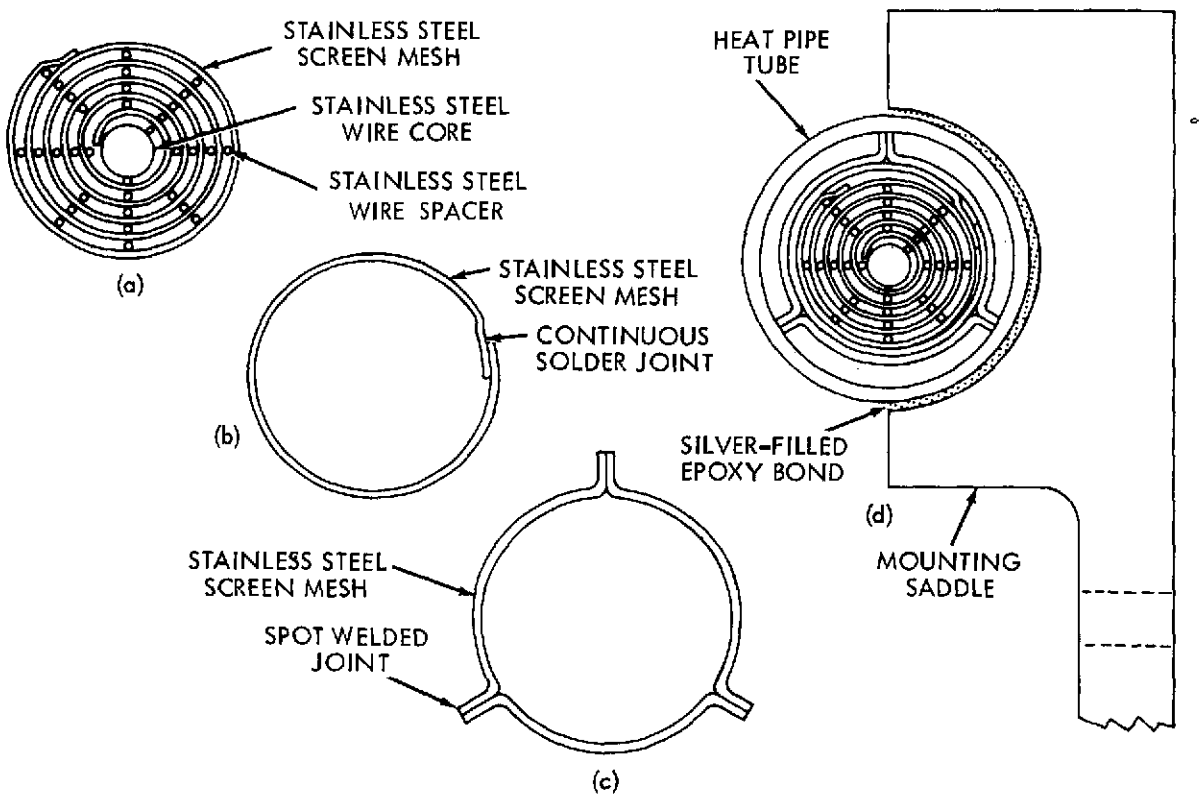

Figure 6. Detailed views of artery wicking device.

Other wires, which serve as spacers, are welded on the mesh at 6.3 mm (1/4 in.) intervals, parallel to the core wire. The whole is then rolled around the core wire Figure 6 (a), to form a wick approximately 3.74 m (147.3 in.) long and 6.5mm (0.255 in.) in diameter.

This wick is enclosed in a cover or sock, Figure 6 (b), also formed of the stainless steel 100 mesh; and this in turn is surrounded by the artery retainer (c), made of the same mesh screen, which supports the wick and makes contact with the outside wall. The entire wick is then forced into the heat pipe tube (d), and the whole is rounded into the shape of a torus of 1.2 m (46.9 in.) diameter, with a nominal 10 cm (4 in.) gap.

There are many reasons for the wicking structure. In addition to helping the return flow of cool liquid to the hot sections of the pipe, the wicking structure provides for better wetting of the entire interior structure. The wicking structure provides the major driving force for the heat pipe, because of the pressure forces which exist across each meniscus, (the curved upper surface of a column of liquid), pressure forces which would not exist without the wick. The wicking structure is used in most heat pipes, the notable exception being a rotating, tapered pipe (Figure 7) which utilizes inertial forces to distribute the

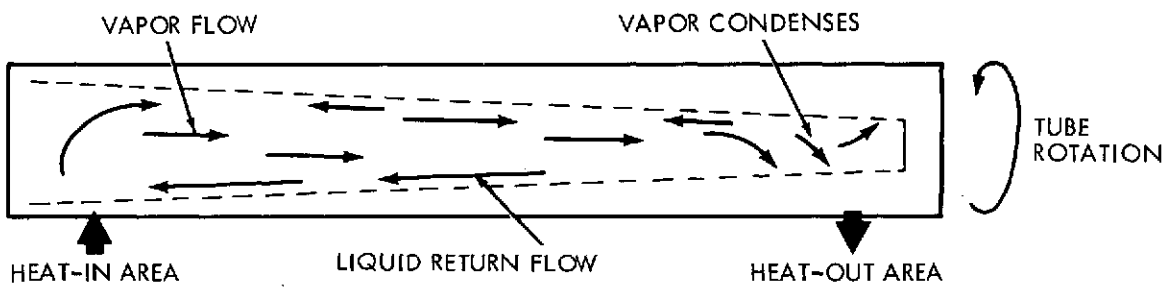

Figure 7. Wickless heat pipe.

working fluid. When used in a 1-G field the rotating type is actually a reflux boiler, in which the liquid flows back to be heated again, and it is not a heat pipe if the heat-in area is lower than the heat-out area.

The mesh screen is commonly used in wicking structures, in both the homogeneous and nonhomogeneous types. The homogeneous type has one type of mesh material and one pore size throughout. The nonhomogeneous type may have different mesh materials or different pore sizes in various parts of the pipe; or the wicking structure may have two layers, one a coarse wire mesh next to the pipe walls, to permit the easier flow of the liquid along the pipe walls, and the other a fine wire mesh on the inside, next to the vapor flow passage, where it produces a large capacity in capillary pumping. Fine mesh increases the capillary pumping capacity, but it also increases the frictional resistance to the movement of the liquid.

Extensive work at the Los Alamos Laboratories indicates that artery-type returns, with the wicking structure, are necessary in the long heat pipes. It was also shown that non-homogeneous wicks worked better than homogeneous wicks.

For fluids other than liquid metals, which were not included in this investigation, good thermal contact between the wicking structure and the walls of the tube is essential for efficient heat transfer and for the minimization of the radial temperature gradients ΔT. The reason is obvious; the better the contact, the lower the thermal resistance. When operating in a zero-G field, a wicking structure of any diameter will fill readily and will coat the walls if enough liquid is available to saturate the wick. This is not the case in a 1-G field, where the gravitational pull prevents the higher portions of the wick from filling as rapidly and completely as the bottom portions of the wick. However, ethyl alcohol in a small diameter (3 mm) tube is an example; this liquid has extremely good wettability characteristics. The degree to which other liquids can fill and coat the walls of larger diameter tubes is proportional to

$$\frac{\sigma}{\rho_\ell}$$

This states that the greater the surface tension and the lower the liquid density, the easier it is for a liquid to rise in the wicking structure in a 1-G field.

Method of Charging a Heat Pipe

Charging a heat pipe with a working fluid is a difficult task because of the necessity of having a clean pipe and a pure, uncontaminated fluid. Extreme care must be taken to ensure that all foreign matter is removed from the pipe prior to charging to prevent a possible chemical reaction which could lead to the generation of a noncondensable gas or to the formation of sludge.

Normally the heat pipe container is cleaned many times, baked out, and evacuated with a vacuum pump. After this, a supply of the working fluid is connected to the evacuated pipe through a vacuum system, and the fluid is slowly leaked into the system until the desired weight of fluid has entered the pipe. Once this occurs, the line connecting the heat pipe to the vacuum system is pinched off and sealed about one-half inch from the pipe. The major danger during any of these steps is the inclusion of gases other than the gas and fluid desired.

HEAT PIPE OPERATION

Heat pipe operation can be described simply, with reference to Figure 8, as follows: The fluid-vapor combination creates a closed, flowing system. Prior to the application of heat, the fluid is in a steady-state, no-flow condition. As heat is introduced in the evaporator section, the local liquid is vaporized, causing a local increase in vapor pressure, which results in a vapor pressure differential along the pipe. This vapor pressure gradient provides the driving force which causes the vapor to flow into the colder or condenser section of the pipe.

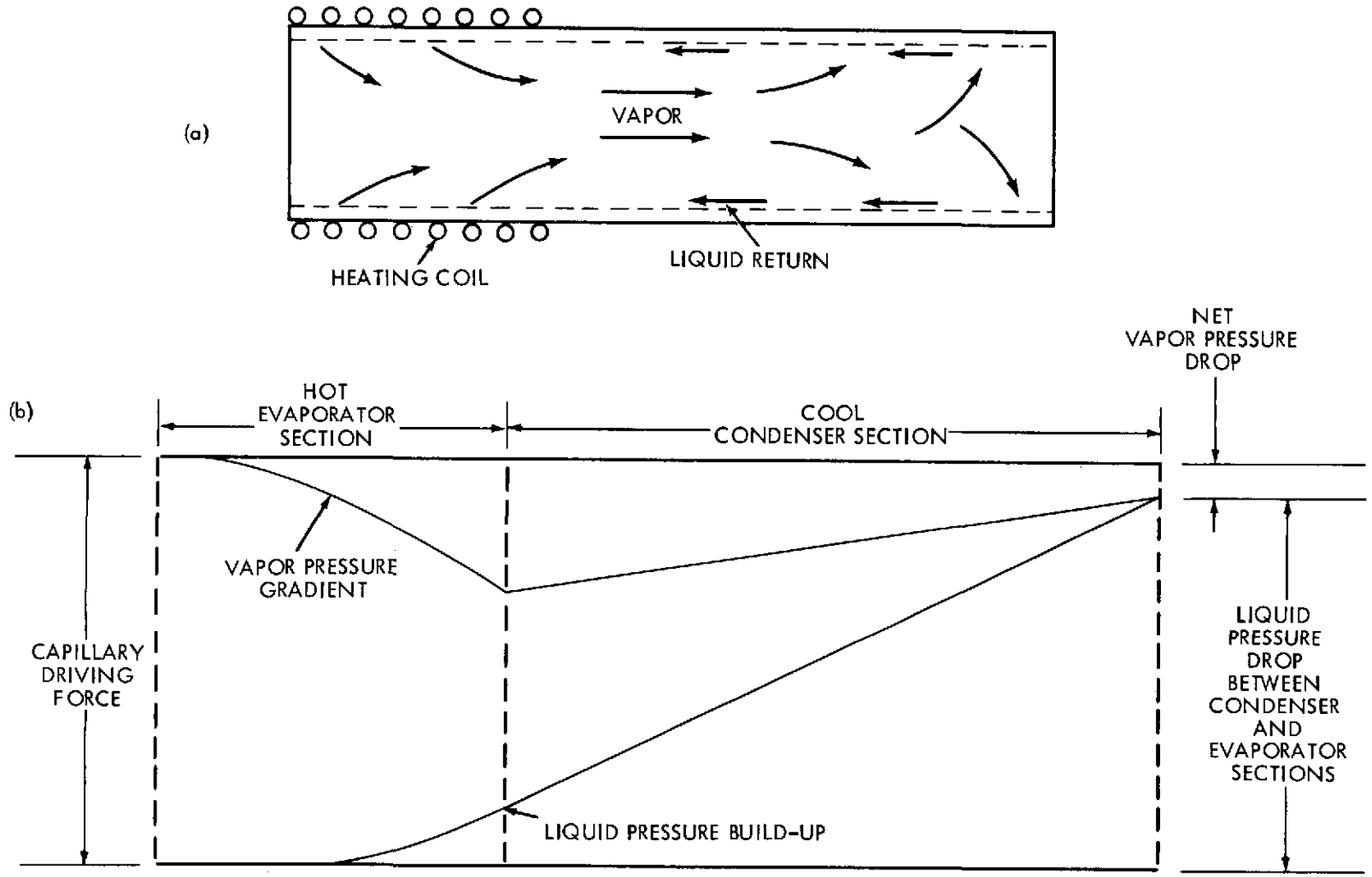

Figure 8. Heat pipe circulation and pressure diagrams.

Once the hot vapor reaches the colder sections of the pipe, condensation occurs, and the liquid returns to the evaporator section by capillary action through the wicking structure or artery. As soon as the vapor begins to condense a liquid-pressure gradient is created, which may, under the influence of gravity, aid the return of the fluid to the hot sections. Since there is virtually no gravitational effect in orbit, this gravitational force is counteracted during testing by placing the heat pipe on the tilt table and providing a slightly uphill path for the liquid return. This also avoids the hydrodynamic head or pressure formed by puddling of the liquid, which could aid the return flow of fluid to the evaporator.

The dominant driving force for the liquid return, the capillary action of the wicking structure, is a result of the fluid surface tension. Even in a 1-G environment and in contact with a solid object, the liquid tends to create minimum surface shapes. These shapes are distorted, however, because of the adhesive forces which exist between unlike substances.

In a heat pipe with sufficient liquid the wick will draw continuously upon the available liquid, in order to continously recreate minimum surface shapes; this is the mechanism and motion called capillary action. This capillary action is always toward the hotter and drier sections. The net result of this capillary action is fluid flow, and under the proper conditions this flow can be rapid.

In a nondynamic, zero-G condition, pipe flow will continue indefinitely as a result of capillary action. As mentioned previously, the flow of the fluid in a vertical direction in a 1-G field will stop when the weight of the liquid column being supported equals the force of gravity acting against it.

In examining the modes of heat transfer, it is noted that three modes can occur; surface evaporation, nucleate boiling, and film boiling. Conduction of heat through liquids and vapors is small, compared with heat conduction through metals. Under controlled conditions, the evaporation of the fluid in heat pipes is accomplished by surface evaporation, which as the name implies is the evaporation of molecules at the liquid-vapor interface. Nucleate boiling is the formation of vapor bubbles around small particles which serve as nuclei. There is strong experimental evidence that this type of boiling can be avoided by using ultraclean fluids in ultraclean pipes.

Film boiling is the condition where a film forms on the surface being heated, such as the bottom of a pan. As the heat input continues or increases, the film layer thickens until its buoyancy force exceeds the surface tension force, causing the film to break away and to rise to the surface of the liquid. Film boiling will not occur in a heat pipe unless local heat inputs create an overdriven condition, causing rapid dryout in the pipe. Dryout is a failure of the system to function, and is to be avoided in all operational cases. As in the case of steam boilers, the design of the heat pipe must be such that film boiling is negated, or large thermal gradients will occur, resulting in dryout of the heat pipe.

Because evaporation and condensation may occur anywhere along the length of the tube,

and are basically independent functions, the heat pipe tends to be a self-regulating and isothermal system. Radial gradients, however, can exist. This is because the cross-sectional areas of the pipes vary due to the porous wicks, causing non-uniform flow patterns. Further, non-uniform contact of the wick with the shell creates additional radial gradients. These gradients can be on the order of several degrees. Since this is basically an internal problem and cannot be measured with available techniques, only the longitudinal gradient is seen and is measureable.

GOVERNING ANALYTICAL EQUATIONS

Pressure Gradient Equations

As indicated above, a heat pipe consists of a sealed tube, a working fluid, and a wicking structure. The wick volume contains the liquid phase of the working fluid, and the remaining volume of the pipe contains the vapor phase. In operation, heat is applied to one section and is removed from another, establishing a two phase, counter-current flow regime. Evaporation and condensation can occur at any place in the pipe where the liquid-vapor interface exists.

The heat input and removal cycle, as mentioned previously, consists of five steps: (1) vaporization of the local liquid in the heat input area; (2) movement of the hot vapor to the cooler section of the pipe; (3) conduction of the heat through the container wall; (4) condensation of the vapor into a liquid; and (5) return of the liquid through the wick to the warm area by capillary attraction.

Fluid circulation in the pipe is thus maintained by the capillary forces which develop in the wick structure at the liquid-vapor interface. For steady operation (see Figure 9) this flow can be expressed in pressure terms as follows:

$$P_{fe} = P_{ge} - (P_{ge} - P_{gc}) - (P_{fc} - P_{fe}) - \text{Gravity forces} \qquad (1)$$

or

$$P_{ge} - P_{fe} = (P_{ge} - P_{gc}) + (P_{fc} - P_{fe}) + \text{Gravity forces} \qquad (2)$$

or

$$\Delta P_c \geq \Delta P_g + \Delta P_\ell + \Delta P_s \qquad (3)$$

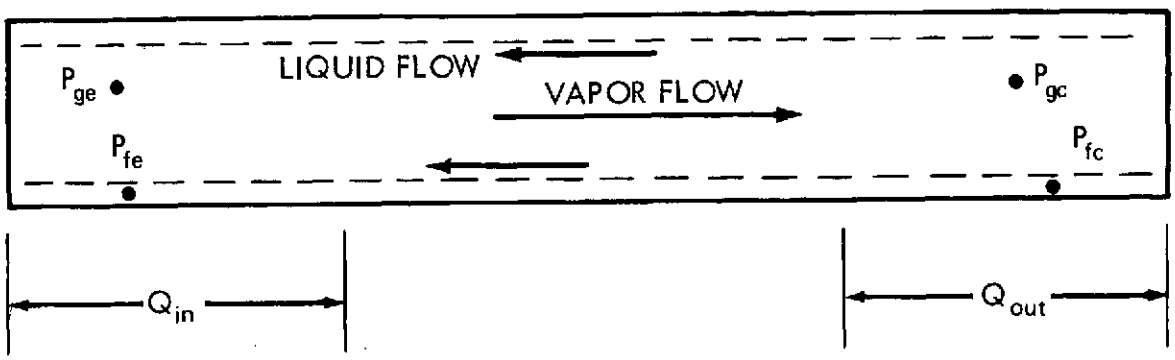

Figure 9. Heat pipe steady operation pressure terms.

where

ΔP_c = capillary pumping pressure

ΔP_g = vapor flow pressure drop

ΔP_ℓ = liquid flow pressure drop

ΔP_s = gravitational force

P_{fe} = pressure of the fluid in the evaporator

P_{ge} = pressure of the gas in the evaporator

P_{gc} = pressure of the gas in the condenser

P_{fc} = pressure of the fluid in the condenser

Equation (3) expresses the necessary capillary pull required for the heat pipe to function. While this equation looks simple, the determination of each quantity is very difficult. A discussion of the first three of these terms follows.

Capillary Pumping Pressure — ΔP_c

The capillary forces have to balance the pressure losses due both to vapor and liquid drag as well as to the gravitational differences when in a 1-G environment. This is accomplished by many tiny menisci, for a screen wick, that form at the vapor-liquid interface. This allows the vapor pressure to be higher than the liquid pressure throughout the heat pipe. For a screen or channel system, a typical meniscus is characterized by two principal radii (r_1, r_2) of curvature. Thus at any point, the pressure drop across the liquid-vapor interface is given by

$$\Delta P_c = \sigma\left(\frac{1}{r_1} + \frac{1}{r_2}\right)\cos\theta \qquad (4)$$

If the working fluid wets the wick completely, θ = 0 degree, this equation yields the maximum capillary force (ΔP_c). This is because once the heat transfer limit is reached, the liquid meniscus will be defined exactly by the wicking structure being used. However, for longitudinal channels the radius of curvature along the major axis of the channel can and does become very large; and, therefore, this radius of curvature is ineffective in determining ΔP_c. Thus only the circumferential radius across the channel is important. For steady-state operations this radius is smallest in the evaporator, because of fluid evaporation, and will decrease with increased heat loads until it approximates half the channel width. When this occurs the limiting heat transfer case has been achieved, and ΔP_c can be expressed as:

$$\Delta P_c = \frac{\sigma}{r} \qquad (5)$$

where r = 1/2 the channel width and θ = 0 degree. If $\theta \neq 0$ degree, $r = r_1 \sec\theta$, where r_1 = liquid radius of curvature. Therefore, if $r_1 = r_2$ in Equation (4), it is shown that ΔP_c max doubles.

Liquid Flow Pressure Drop – ΔP_ℓ

Equations to express the liquid pressure drop along the pipe are much more complex than those used to express ΔP_c, but some simplifying assumptions can be made. The most useful of these assumptions is that the radial pressure differences are much less than the axial-length pressure gradients. This in general is a valid assumption, because the axial length of the pipe, L, is much greater than its radius, r_p. Poiseuille's equation is useful for expressing the liquid pressure drop through a capillary tube. This is given as

$$\Delta P_\ell = \frac{8\mu_\ell \dot{m}_\ell L}{\pi r_p^4 \rho_\ell} \qquad (6)$$

where

μ_ℓ = liquid viscosity

$\dot{m}_\ell$ = liquid mass flow rate

L = tube length

ρ_ℓ = liquid density

r_p = tube radius

Equation (6) can be re-expressed for the cross sections of the pipes shown in Figure 5.

(a) Artery
$$\Delta P_\ell = \frac{8\mu_\ell Q L_e}{\pi r^4 \rho_\ell h_{fg}} \tag{7}$$

(b) Channels
$$\Delta P_\ell = \frac{8\mu_\ell Q L_e}{\pi r_e^4 N \rho_\ell h_{fg}} \tag{8}$$

(c) Screen
$$\Delta P_\ell = \frac{b\mu_\ell Q L_e}{\pi (R_w^2 - R^2) \epsilon r_c^2 \rho_\ell h_{fg}} \tag{9}$$

(d) Concentric Annulus
$$\Delta P_\ell = \frac{12\mu_\ell Q L_e}{\pi D W^3 \rho_\ell h_{fg}} \tag{10}$$

(e) Crescent Annulus
$$\Delta P_\ell = \frac{4.8\mu_\ell Q L_e}{\pi D W_e^3 \rho_\ell h_{fg}} \tag{11}$$

where

L_e = effective heat pipe length

r_e = effective channel radius

N = number of channels

b = screen tortuosity factor

R_w = outer radius of screen

R = vapor flow passage radius

ϵ = screen void fraction

r_c = effective radius of screen openings

D = mean diameter of annulus

W = width of annulus

Q = rate of heat transfer from one section to another section of the heat pipe

h_{fg} = latent heat of vaporization

W_e = effective width of annulus

Vapor Flow Pressure Drop $-\Delta P_g$

Vapor flow in the evaporator and condenser sections of the pipe is dynamically identical to pipe flow with injection or suction through a porous wall, and is a function of the Reynolds number. If the Reynolds number is $<<1$, viscous effects dominate the inertial effects of the flow, and Equation (6) can be used to determine the vapor pressure drop along the pipe.

$$\frac{dP_f}{dL} = \frac{-8\,\mu_v \dot{m}_v}{\pi\,\rho_v\,r_v^4}\left(1 + \frac{3}{4}R_e - \frac{11}{27}R_e^2 + \ldots\right) \tag{12}$$

where

μ_v = vapor viscosity

$\dot{m}_v$ = vapor mass flow rate

ρ_v = vapor density

r_v = vapor flow radius

R_e = Reynolds number

The negative sign is used since the pressure decreases along the flow path.

Equation (12) is the result of assuming a Poiseuille flow pattern with an expanded perturbation expression used for the velocity. This is used because it is known that in the evaporator and condenser sections of the heat pipe the velocity profile departs from that of Poiseuille flow.

When evaporation rates are high ($R_e >> 1$ but < 2000) and the flow becomes boundary layer flow, the pressure begins a dynamic recovery in the condenser sections. For this case, the following equation is used:

$$\frac{dP_f}{dL} = \frac{-S m_v}{4\,\rho_v\,r_v^4}\left(\frac{dm_v}{dL}\right) \tag{13}$$

where $S = 1$ for the evaporator sections and $4/\pi^2$ for the condenser sections.

If fully turbulent flow develops, the empirical Blasius equation can be used to express ΔP_v. This is given by:

$$\frac{dP_f}{dL} = \frac{-0.0655\,\mu_v^2\,R_e^{7/4}}{4\,\rho_v\,r_v^3} \tag{14}$$

This equation should be used when $R_e > 2000$.

Thus a major gap exists between the flow regions covered by Equations (12) and (13); that is, the case for $R_e = 1$ is not covered. Further, since the velocities are extremely difficult to measure, the R_e cannot be accurately determined, and the appropriate equation to be used is questionable. The Reynolds number is given as:

$$R_e = \frac{\rho_\ell D V}{\mu_\ell}$$

which can be re-expressed as

$$R_e = \frac{\dot{m}_v}{\pi r_v \mu_v}$$

where

D = pipe diameter

V = average velocity across the vapor flow passage

Thus we are stranded analytically with three equations. However, pipe flow experiments other than those with heat pipes have enabled the determination of the onset of turbulence as a well-defined function of the Reynolds number. These results are: If $R_e > 1000$ and $L > 50\, r_p$, use Equation (13); if $R_e > 2000$, use Equation (14).

An extension of these analyses to include a method to determine ΔP_c from simpler tests, expressions for the mass flow rates, boundary conditions, and heat transfer equations follows.

Equations of Motion, Continuity, and Heat Transfer with Boundary Conditions and Flow Limitations

In any convective heat transfer situation, a minimum of three equations are necessary to describe the problem. These are (1) the equation of motion, (2) the continuity equation, and (3) the governing heat transfer equation. With a complete set of boundary conditions, an analytical solution can be achieved if the governing equations are of sufficient simplicity. For heat pipe analysis and understanding, the equations of motion are given along with the hydrostatic equation, since gravity effects in a 1-G field can be great in the first case and the only factor in the latter. Velocity boundary conditions are presented; and mass flow rate equations, thermal gradients equations, and a list of flow inhibitions and limits are also included to aid in a more complete understanding of the situation.

Equation of Motion

The equation of motion is actually three equations, but can be written in vector form as:

$$\frac{D\vec{v}}{Dt} = \frac{-\nabla p}{\rho} + \mu\nabla^2\vec{v} + \vec{g} \tag{15}$$

where D ( )/Dt is the substantial or material derivative, which is expressed as:

$$\frac{\partial(\ )}{\partial t} + \frac{u\,\partial(\ )}{\partial x} + \frac{v\,\partial(\ )}{\partial y} + \frac{w\,\partial(\ )}{\partial z}$$

The hydrostatic equation is evolved when $\vec{v} = 0$:

$$\nabla p = \rho\,\vec{g} \tag{16}$$

If we assume $\vec{g}$ acts only in the vertical direction; i.e., $\vec{g} = g_0\,\hat{h}$, Equation (15) becomes

$$\nabla p = h\,\rho\,g\sin\phi = \Delta P_g \tag{17}$$

where ϕ = pipe tilt angle departing from a horizontal position.

ΔP can also be expressed as the difference in static pressure due to the weight of liquid between two sections in the pipe. Gravitational effects are assumed zero for the vapor flow sections, and for analytical purposes the gas is assumed to have a Boltzmann distribution in a 1-G field. The pressure difference would be a maximum between the two pipe ends. Since the gravitational effects can be evaluated rather easily, a simple method to determine ΔP_c in a static conditon can be achieved.

Analytical Determination of ΔP_c

Figure 10 shows a typical liquid profile supported by the wicking structure of the heat pipe. As noted, the liquid profile is not necessarily uniform. However, across each of the local liquid-vapor interfaces a pressure balance exists. This can be shown to be equal to

$$P_v(L) - P_\ell(L) = \frac{2\sigma}{r(L)} \tag{18}$$

Equation (18) is a function of position as noted. Now, in a static state, all pressure

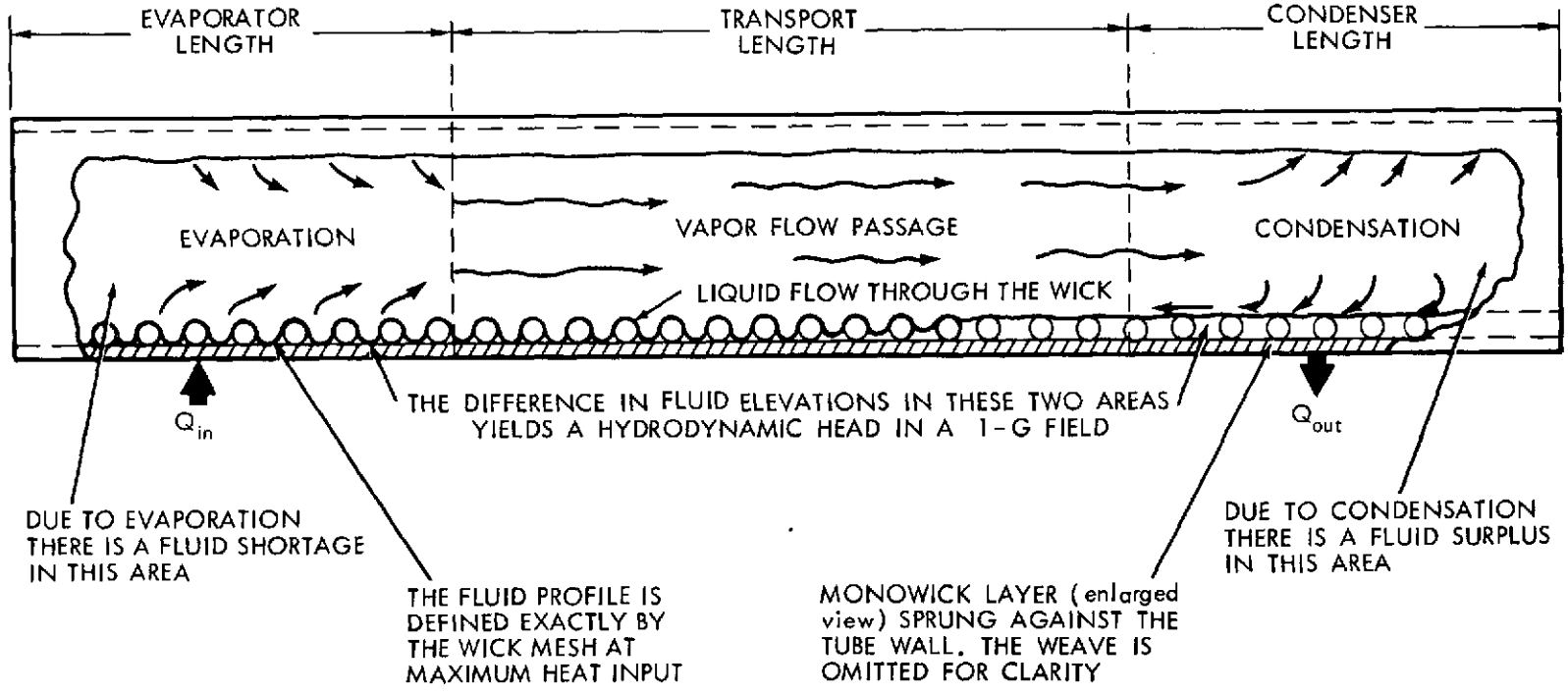

Figure 10. Heat pipe vapor–liquid interface.

differences are equal. Thus, equating Equations (17) and (18) and solving for h yields

$$h_{max} = \frac{2\,\sigma \cos\theta}{\rho_\ell g\, r_c \sin\phi} \tag{19}$$

where

$$r\,(L) = r_c\,(L)/\cos\theta$$

Equation (19) provides an analytical expression which can be used to predict ΔP_c (Note: $\Delta P_c = \rho g h_{max}$). This can be checked experimentally under static conditions by the diagram shown in Figure 2. For a steady-state operating pipe, r_c varies along the pipe. If θ is assumed to be zero degree, the only problem in solving equation (19) comes about in the value used for r_c. This radius, r_c, a variable, is minimized in the hot sections of the pipe as the liquid is depleted. Thus, r_c approaches one-half pore diameter of the wire mesh in the evaporator sections of the heat pipe as the maximum heat transfer rate is approached. This is exactly true for a circle.

In the cold sections of the pipe the radius of curvature, r_c, approaches infinity if there is excessive fluid buildup of condensed fluid.

Boundary Conditions and Mass Flow Rates

The conservation of mass equation can be expressed in vector form as:

$$\nabla \cdot \rho \vec{V} = 0 \tag{20}$$

where

$$V = V\,(L, r_w) = V\,(0, r) = V\,(L, r) = 0$$

In other words, the velocity at the walls and at the tube ends is zero. (See Figure 11.) Now assuming that the vapor density is given as $\rho_v\,(L, r)$ and that the velocity is given as $V_v\,(L, r)$, the vapor mass flow rate can be expressed as

$$\dot{m}_v\,(L) = \int_0^{r_v} \rho_v\,(L, r)\, V_v\,(L, r)\, 2\,\pi\, r\, d\, r \tag{21}$$

where

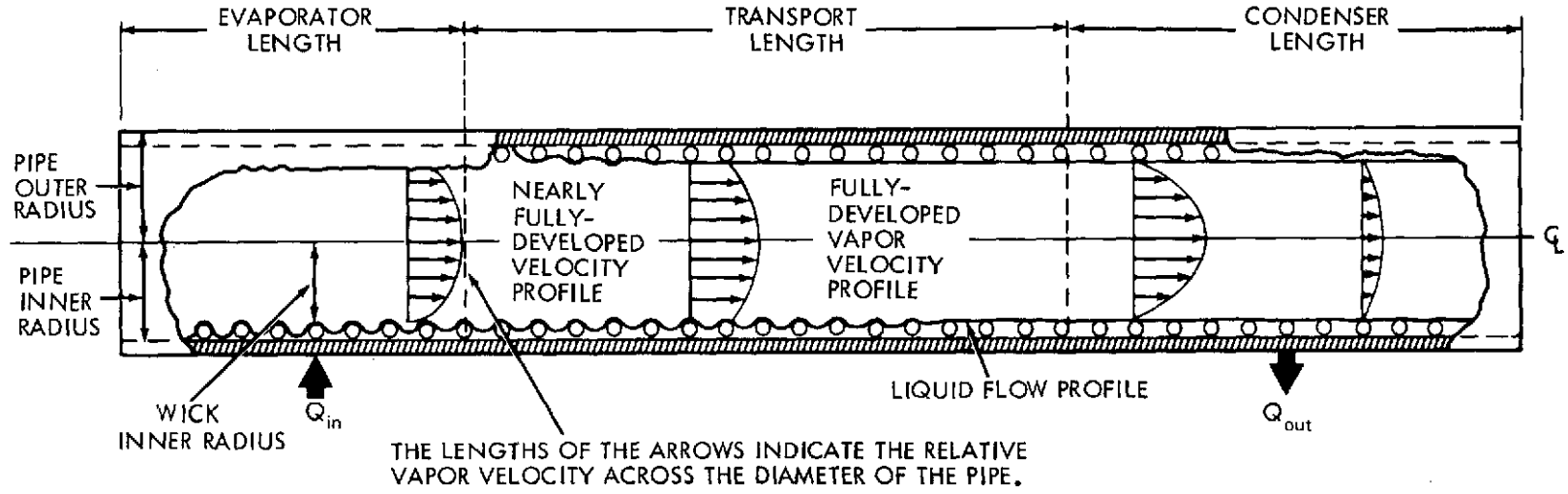

Figure 11. Vapor velocity profile within a heat pipe.

r_w = wall or wick radius

r_v = vapor flow passage radius

Likewise an expression for the mass flow rate in the liquid phase can be expressed as

$$\dot{m}_\ell(L) = \int_{r_v}^{r_w} \rho_\ell(L, r)\, V_\ell(L, r)\, 2\pi r\, dr \tag{22}$$

and based on the conservation of mass principle:

$$\dot{m}_\ell(L) + \dot{m}_v(L) = 0 \tag{23}$$

Therefore, once either of the mass flow rates has been determined the other is also determined.

Heat Transfer

For the steady-state transportation of heat, the energy equation can be written in vector form as:

$$\nabla \cdot \vec{Q} = 0 \tag{24}$$

where

$$\vec{Q} = h\rho\vec{V} - k\nabla T \tag{25}$$

By definition, the heat pipe functions when the axial and radial thermal gradients are small, even though the heat transport may be large. Axial conduction is neglected, since the heat pipe has small wall thickness. Therefore:

$$Q = \int_0^{r_v} h_v \rho_v V_v\, 2\pi r\, dr + \int_{r_v}^{r_w} h_\ell \rho_\ell v_\ell 2\pi r\, dr \tag{26}$$

Substituting for the mass flow rates yields

$$Q = h_{fg}\ \dot{m}_V\ (L) \tag{27}$$

Thus it is seen that the axial transport of heat is maximum at the end of the evaporator, and can be expressed as the product of the latent heat of vaporization times the mass flow rate.

Thermal Gradients

A simple relationship that aids in theoretically determining the vapor temperature from the pipe temperature is given by

$$T_p = T_v + H_T/K \tag{28}$$

where

H_T = heat added per unit length in the evaporator

and

$$\frac{1}{K} = \frac{1}{2\pi}\left[\frac{1}{K_p}\ \ell n\ \left(\frac{r_p}{r_w}\right) + \frac{1}{K_w}\ \ell n\ \left(\frac{r_w}{r_v}\right)\right] \tag{29}$$

where

r_p = pipe radius

K_p = thermal conductivity of the pipe

K_w = thermal conductivity of the wick

The temperature drops in the vapor section of the heat pipe can be obtained by using the Clapeyron-Clausius equation:

$$\Delta T_v = T_v\ (L) - T_v\ (0) = \frac{R\ T_0^2\ \Delta P}{M\ h_{fg}\ P\ (T_0)} \tag{30}$$

where ΔP is small. This equation is good when the pipe is completely wet, has small thermal gradients, and utilizes nothing but surface evaporation to complete the change of state from liquid to vapor.

Flow Limitations: Entrainment

If a heat pipe is functioning properly, its maximum heat-carrying capacity can be achieved. This occurs when the flow is stable, the wick is completely wet, no hot spots exist, and small pressure gradients serve as the driving forces for liquid and saturated vapor flows.

Any slight departure or perturbation of this balanced flow condition by excessive heating rates could cause liquid drops to form in the vapor flow passage and could lead to a condensation shock. If a shock should occur, two-phase flow in the vapor channel would result. To lessen the possibility of two-phase flow in the vapor passage, it is essential to limit large areas of liquid surface from high vapor-velocity flow regions. Thus if capillary grooves are aligned in the flow direction, such as in the OAO-B and ATS-F grooved pipes, and are unprotected, a thermal limit due to condensation shock could occur.

The entrainment of liquid drops into the vapor flow passage is due to dynamic instability at the liquid-vapor interface. According to linear theory, a given vapor of density ρ_v, flowing at a velocity of V_v past a nearly stationary liquid with surface tension (σ), will create a small amplitude wave which departs from the normal surface with wavelength λ and will grow exponentially with time if

$$\frac{\rho_v V_v^2 \lambda}{2 \pi \sigma} > 1 \qquad (31)$$

Equation (31) is the ratio of dynamic forces to surface tension forces, and is called the Weber number. This equation is a measure of the capture of liquid drops in the vapor flow passage from wave crests caused by the perturbated conditions. This condition, if achieved, will cause the heat pipe to stall and the evaporator to overheat. Experimentation to date has shown that the use of fine mesh wire wicks tends to prevent liquid capture.

Other Heat Flow Limitations

Other limitations are (1) overheating (local hot spots) in the evaporator sections due to lack of sufficient liquid return; (2) insufficient return of liquid as limited by the capillary pumping mechanism; (3) limits due to counter current shear at the liquid-vapor interface; and (4) sonic limit, choke flow.

TEST CONFIGURATION

Based upon knowledge of how heat pipes work, analysis of test data can be interpreted to yield intricate details of functionability. To obtain these details, it is essential to have a flexible test setup.

As shown in Figure 12, the test configuration for each of the high-power heat pipes

included a mobile tilt table, on which the individual pipes were mounted on teflon standoffs, with two flight heaters, four test heaters, and numerous thermocouples to monitor the temperature. In the center foreground is shown the vacuum rated motor used to change the relative elevations of the evaporator and condenser sections of the

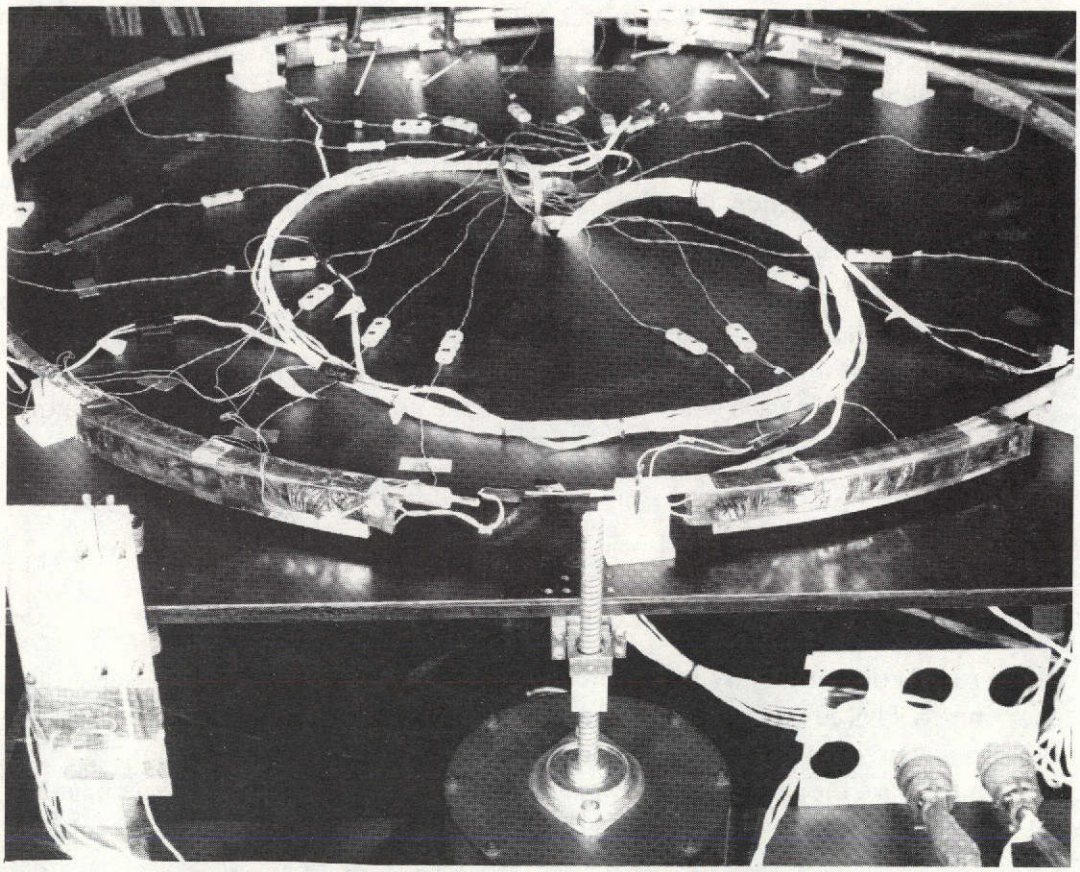

Figure 12. Test configuration: heat pipe mounted on tilt table.

heat pipe, with a 3.8 cm (1-1/2 in.) tilt available. Also shown in the foreground are two of the test heaters, attached to two of the heat pipe mounting saddles and wrapped in insulation. The lines from the thermocouples were run to recorders through a central hole in the table top.

The table with the mounted heat pipe and equipment was then pushed into the thermal vacuum chamber, as shown in Figure 13, for the tests. At the left rear of the vacuum chamber may be seen the pipes from the Conrad cooling unit, used to lower the temperature of one or both condenser sections of the tube. This heat removal system

operates between −65° C and +50° C with a controllable accuracy of ±2° C. The chamber was established at a vacuum of approximately 10^{-7} torr, and the cold walls were controlled from −40° C to +20° C.

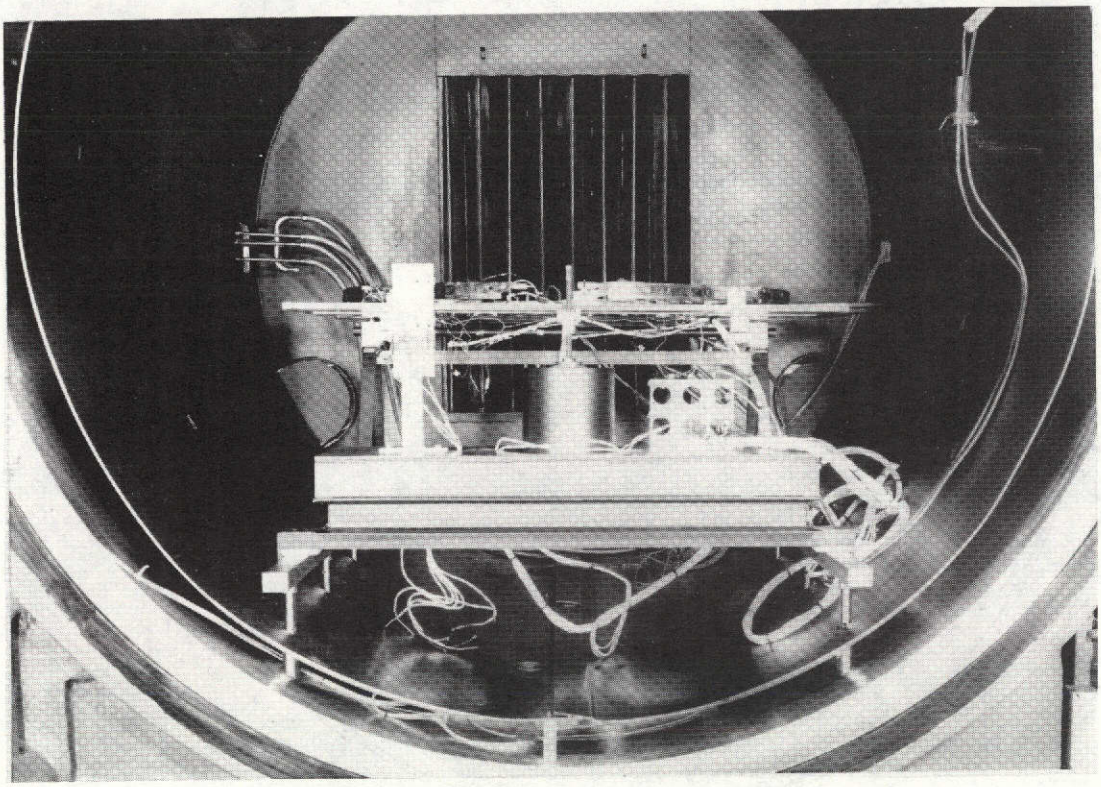

Figure 13. Thermal vacuum chamber setup.

The locations of the test and flight saddle heaters and of the 18 thermocouples are shown in Figure 14. The thermocouples were placed to monitor the heat pipe temperatures and also the operation of the heaters and of the Conrad cooling lines to the condensers. Power levels for the test heaters could be varied from 0 to 100 watts; for flight heater Number 1, from 0 to 50 watts; and for flight heater Number 2, from 0 to 25 watts. Cross sections of the heat pipes tested are shown in Figure 5 (a-1) and (a-2) and in Figure 6.

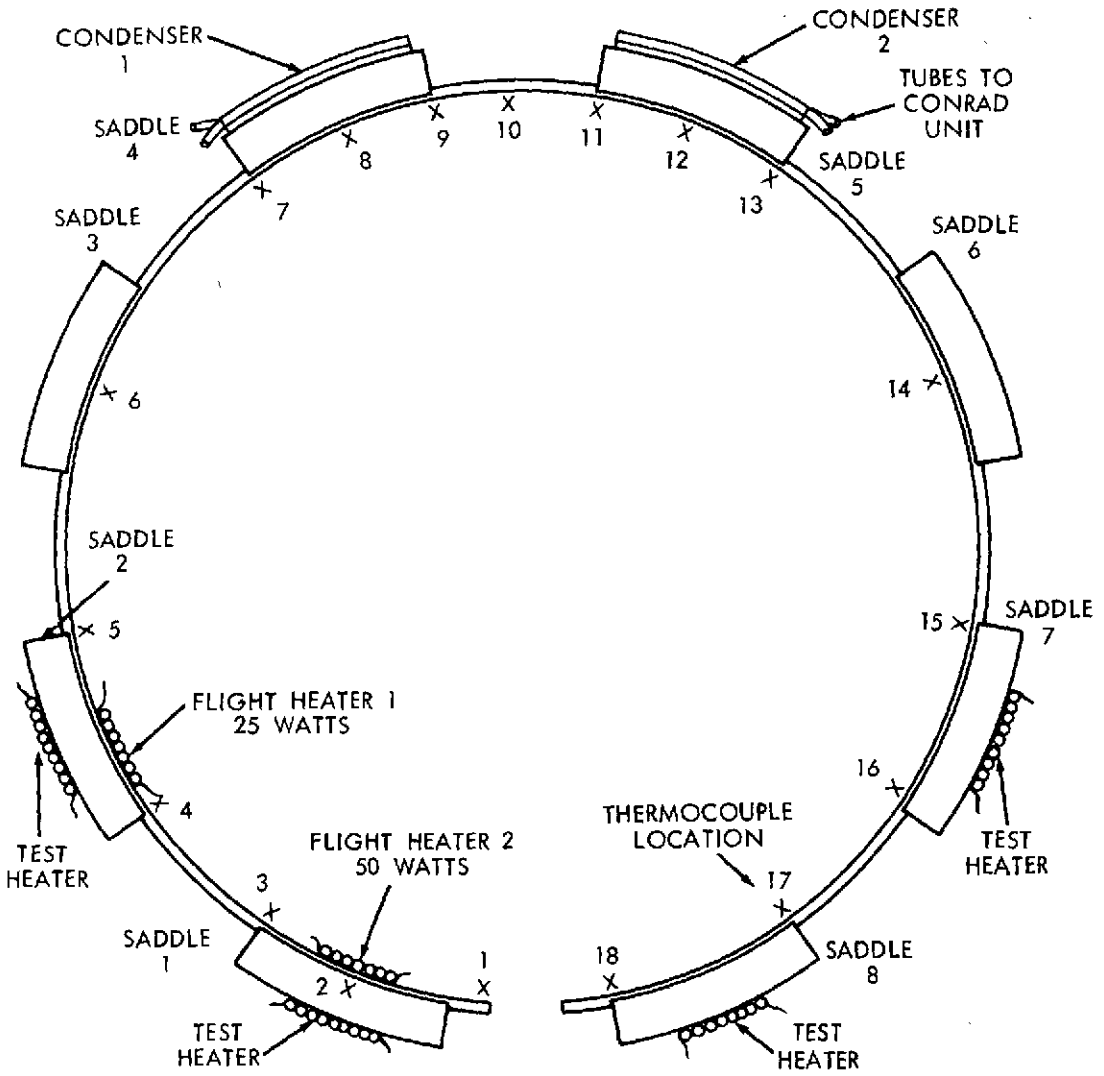

Figure 14. Locations of heaters, condensers, and thermocouples.

TEST RESULTS AND CONSIDERATIONS

Performance Requirements

Heat pipes are of great value if they are designed and constructed with extreme care. Mathematical models exist today, but nothing works perfectly all the time, and thus thermal vacuum and bench testing become essential. Since most pipes will be required to operate for 12,000 or 20,000 hours and longer, in a vacuum and under wide temperature extremes, it is essential that rigorous testing for performance and material compatibility be conducted.

The generation of even a small amount of hydrogen gas in an ammonia or freon heat pipe can create a binary gas situation which results in poor pipe performance. This is a direct result of the light hydrogen gas being swept down the pipe by vapor pressure differences.

Once in the condenser sections of the pipe, the hydrogen gas blocks a portion of the condenser, and prevents condensation of the working fluid along the condenser. If the heat pipe is blocked, the evaporator sections become warmer and the condenser sections become colder, resulting in large gradients which defeat the purpose of the heat pipe. A tiny quantity of water vapor, as little as 50 parts per million, can completely ruin the functioning of a heat pipe. The inclusion of hydrogen gas was shown recently to be the cause of the failure of an OAO-C heat pipe while it was undergoing a thermal vacuum test.

The water vapor probably entered the pipe while the pipe was being sealed. The problem was corrected by emptying, cleaning, and carefully recharging the tube. The retesting of this pipe, which was flown on the OAO-C spacecraft, was successful. Hydrogen gas problems also occurred with the ATS-F internally grooved pipes. In that instance the source of the hydrogen gas was not determined, but it might have been generated by a reaction between the ammonia and a solvent residue left in the pipe. These difficulties with hydrogen gas indicate that while heat pipes have the ability to isothermalize the structure they surround, their functioning is very sensitive to cleanliness, to the purity of the working fluid, and to the fluid/container compatibility.

Basic Test Philosophy and Goals

The OAO-C heat pipes were tested under thermal vacuum conditions to provide a means of evaluating two performance requirements; (1) the degree of isothermalization required under all test conditions, and (2) the high heat transport capability, which greatly exceeds the requirements of the mission. Necessary conditions for high performance are that the fluid must prime the artery and that bubbles formed in the artery must readily dissolve.

A considerable amount of data and experience were obtained in testing the OAO-C spacecraft heat pipes. The basic test goals for the OAO heat pipes are similar to the test goals for other heat pipe systems, and therefore only the OAO pipes are discussed.

Ground Test Results

Long Periods for Temperature Stabilization

One of the first and most noticeable differences realized under the thermal vacuum testing of the two high-power OAO-C pipes was the length of time required to stabilize the pipes. Thermal vacuum stabilization periods were on the order of four to six times as long as bench testing times.

Higher Delta Temperatures

A second difference was that the delta temperatures (ΔT's) recorded during vacuum testing were higher than those recorded on the bench. This was probably due to convection on the bench, even though the pipes during the bench testing were insulated. Since tilt tests were performed and the data were carefully recorded, good accuracy as to stabilization points was achieved.

Effects of Tilt

It was noticed that the overall pipe ΔT's were lower at a 0.64-cm tilt (the evaporator always above the condenser) than at the level test condition. This occurred in approximately 70 percent of all test conditions. This may be due to the effects of hydrodynamic puddling on the fluid flow, but more testing on other heat pipes is required to confirm this conclusion. This problem will be investigated further during the testing of the ATS-F pipes at Goddard.

Burnout and Repriming

It was also demonstrated that as the tilt was increased, the ΔT's in general changed very little up to the point of burnout, and in most cases there was no indication prior to burnout that the pipe would cease to function. This indicated that the wick design is excellent, and that the wick is capable of carrying large heat loads without large thermal gradients. Burnout occurs when the wicking structure in the heat-input area finally becomes unable to supply fluid as fast as it is evaporated, which causes the heat input area to become dry and the local temperature to start a rapid rise. A typical example of this sudden burnout condition is shown in Table 1. For this test the chamber was under vacuum, the chamber walls were at $-40°$ C, and the condenser was conditioned by the heat removal unit at $-55°$ C. Looking at the overall pipe ΔT's in column 4 of Table 1, it will be noted that little if any change was recorded as the tilt was increased. Table 1 gives the result of the thermal vacuum test of the OAO-C spiral artery heat pipe, when only the flight heaters were used. Highlighting the importance of the heat removal effects, it will be noted that there was a considerable difference in pipe performance when the condensers were changed from $-55°$ C to $-40°$ C, also shown in Table 1. This indicates that under some test conditions the condenser temperature is the controlling factor.

Burnout, in which one section of the pipe becomes very hot, was also characterized during the tests by the remaining portions of the pipe becoming slightly cooler, since the heat removal mechanism continually removed heat from the fluid and vapor near the condenser.

Once burnout has occurred, the heat pipe must show the ability to reprime. The technique used during the tests at Goddard to restore the pipe to proper functioning after burnout is as follows: If the pipe is in a tilted position when burnout occurs, all power is turned off and the pipe is allowed to recover in this position. After low ΔT's, approximately $1°$ to $2°$ C, have been established the pipe is releveled and is allowed to remain in this position for approximately 30 minutes. This procedure has worked in all the burnout cases tested so far. When the pipe is left in a tilted position, gas bubbles are readily formed and dissolved. As the liquid inches up the pipe it tends to form trapped gas pockets, which are lighter than the liquid, and these gas pockets are pushed from the colder toward the warmer areas, allowing them to condense or dissolve.

On the other hand, if a large gas pocket is trapped after burnout, when the pipe is in the level position, it may be overwhelmed by a large amount of fluid, and then the pipe will require a lengthy recovery time, since some noncondensable gases, such as hydrogen, may be present and trapped. This situation would result in a partial recovery only, and it causes poor thermal performance, i.e., large ΔT's. The tilted recovery method is used also because the pipes must be able to reprime in their burnout positions, to indicate the ability of the pipe to function properly in a 1-G field and in space.

Table 1

Flight Heater Data.

Heater Power (watts)	Pipe Tilt (centimeters)	Pipe Average Temperature (°C)	ΔT (° C)
Chamber Walls at −40° C; Condensers at −55° C			
25	0	−42.0	0.4
50	0	−37.0	1.0
75	0	−32.0	1.0
25	0.64	−40.0	0.4
50	0.64	−35.5	1.0
75	0.64	−29.5	1.0
25	1.27	−41.0	0.4
50	1.27	−35.0	1.3
75	1.27	−29.0	1.0
25	1.91	−41.5	1.0
50	1.91	−37.0	1.0
75	1.91	–	*[1]
Chamber Walls at −40° C; Condensers at −40° C			
50	1.27	−24.5	1.2
50	1.91	−24.0	1.1
75	1.91	−18.0	1.6
25	2.54	−27.5	0.5
50	2.54	−23.5	3.0
75	2.54	−16.0	3.0[2]

ΔT = Temperature difference between evaporator and condenser sections.

* Burnout: Interior wall becomes dry due to heating rate exceeding the fluid return rate.

[1] Pipe was allowed to reprime and burnout recurred under the same test conditions.

[2] Theoretical ΔT limit approached.

Cool-out and Overheating

Two other types of failures also occurred during testing. The first type is denoted as a cool-out, and the second as overheating. A cool-out occurs when the heat pipe is working well, that is, with low ΔT's. As the heater power is increased to high limits, using the test heaters only, and while the tilt on the pipe is increased, as shown in Table 2, fluid collects in the colder portions of the pipe, insulating the wall and causing a cold spot. Thus, even though the pipe is working well a large gradient can occur in the condenser section of the pipe, causing an out-of-tolerance condition.

Cool-out can occur in more than one location if more than one heat rejection area (condenser) is being used. This results in stable pipe temperatures but high thermal gradients. When a pipe was left in this stable, cool-out condition for several hours it showed no signs of burnout or change.

Overheating, on the other hand, occurs at elevated temperatures. What happens in a case such as this is that the fluid heat transfer property begins to decrease, i.e., the ability of

Table 2

Test Heater Data.

Chamber Walls at −40° C; Condensers at −40° C			
Heater Power per Saddle (watts)	Pipe Tilt (centimeters)	Pipe Average Temperature (° C)	ΔT (° C)
5	0	−35.0	0.5
15	0	−32.0	0.8
25	0	−30.5	0.8
35	0	−29.0	1.3
40	0	−26.0	3.0
70	1.91	12.0	6.0
80	1.91	17.0	8.0
10	2.54	−27.0	2.0
30	2.54	−13.0	3.5
50	2.54	0.0	4.0
70	2.54	11.5	8.0[1]
80	2.54	16.5	16.5[1]

[1] High ΔT caused by condenser cooling dropout, not by overheating.

the fluid to carry large heat loads diminishes greatly. Thus the temperature of the evaporator section of the heat pipe becomes higher than the rest of the pipe. This is

distinctly different from burnout, which is characterized by a local highly elevated temperature in the evaporator section of the heat pipe while the remaining evaporator area of the heat pipe remains relatively cool.

There is no way to distinguish between these two conditions without careful analysis of the data. Thus when ΔT test data is recorded, it is necessary to explain the reason for large ΔT's.

Effect of Environment

Tables 3 and 4 show that even for a good heat pipe system the environment does have some effect on the overall pipe performance, as shown by the slightly higher ΔT's as the overall pipe temperature is elevated by its environment.

The typical test results given in Tables 1 to 4 show that high-powered pipes with low ΔT's can be built, that these heat pipes can aid in the isothermalization of spacecraft

Table 3

Flight Heater Data.

Chamber Walls at 0° C; Condenser at 0° C			
Heater Power (watts)	Pipe Tilt (centimeters)	Pipe Average Temperature (° C)	ΔT (° C)
25	0	9.0	1.0
50	0	14.0	1.0
75	0	20.1	1.0
25	0.64	8.5	0.5
50	0.64	14.0	0.5
75	0.64	19.0	0.5
25	1.27	9.0	0.5
50	1.27	14.5	1.0
75	1.27	20.2	0.9
25	1.91	10.0	0.1
50	1.91	14.8	0.6
75	1.91	21.0	1.2
25	2.54	9.6	0.4
50	2.54	15.0	1.2
75	2.54	21.1	1.8

components in gravitational fields; and that the pipes should function even more effectively under zero-gravity conditions.

Table 4

Flight Heater Data.

Chamber Walls at +20° C; Condenser at +20° C			
Heater Power (watts)	Pipe Tilt (centimeters)	Pipe Average Temperature (° C)	ΔT (° C)
25	0	28.0	0.7
50	0	32.0	0.7
75	0	37.1	0.9
25	0.64	27.2	0.5
50	0.64	31.6	0.9
75	0.64	37.3	0.7
25	1.27	28.0	0.6
50	1.27	32.4	0.8
75	1.27	37.1	0.9
25	1.91	28.0	0.4
50	1.91	32.7	1.0
75	1.91	38.3	1.5
25	2.54	28.0	0.9
50	2.54	32.0	1.9
75	2.54	36.9	2.1

Spacecraft Systems Tests and Flight Data Comparisons

Spacecraft Systems Tests of the OAO-C Heat Pipes

As noted previously, the OAO-C spacecraft has three ambient-type heat pipes. Test results for each of these pipes during the final thermal-vacuum (FTV) spacecraft tests were significantly different from the results obtained from the subsystem bench and thermal-vacuum tests. These differences occurred because an active cooling unit was used to remove heat during the subsystem tests, but in the spacecraft tests cooling was accomplished by radiative and conductive means. This difference does not invalidate the subsystem tests since high-performance requirements had to be proven; whereas, in the spacecraft tests only low-power performance tests were required to prevent overheating in the spacecraft. Thus, overall performance comparisons between the subsystem tests and the spacecraft tests could only

be made when the vapor temperatures and power levels could be matched. Data for these few cases compared favorably.

Flight Experiment Tests

Once the spacecraft was placed into orbit, a series of zero-G tests were completed. These power and spacecraft conditions were as identical to the FTV tests as possible. In all cases the heat pipe flight-heater power levels were regulated by the spacecraft's battery voltage level. The heat pipe flight tests conducted during this time represent the most comprehensive zero-G experiments performed to date. Four separate tests have been conducted and more are anticipated during the projected lifespan of the spacecraft. Some data comparisons from the second and third tests are presented and compared with spacecraft thermal-vacuum test results in Tables 5, 6, and 7. These tables represent a final thermal-vacuum spacecraft ground test and flight test for each of the three ambient-type heat pipes.

OAO-C Spacecraft Description

The OAO-C spacecraft is an octagonal cylindrical hull approximately 305 cm high, with an experiment cavity nearly 125 cm in diameter extending from top to bottom. The cylindrical hull (s/c body) is divided into six levels, or tiers, and the three heat pipes are mechanically attached to the cavity wall in eight places on the lower three tiers (4, 5, and 6). The spacecraft's main experiment is then inserted into the cavity, forming an annulus-type enclosure for the three heat pipes.

Discussion of Flight and Ground Test Data Results

To date, four series of flight tests have been completed. Only data from the second and third series are discussed; however, there was close correlation among all four sets of data. Since flight instrumentation channels were hard to obtain, the number of data channels for the flight tests was greatly reduced from the number used for the ground tests. The ground test instrumentation was supplemented by thermocouples; all flight recorders were thermistors. The flight thermistor positions remained unchanged from the FTV to orbit.

Level 4 Heat Pipe Flight Data

The level 4 heat pipe data are given in Table 5. A cross-sectional view of this pipe is shown in Figure 5(b). By carefully manipulating the heater system during the final thermal-vacuum and flight tests it was possible to make a direct comparison of this pipe's performance at peak heater(s) dissipation with data taken on flight days 25 and 66. Good comparisons between flight and FTV tests were recorded at all power levels.

It is noted in Table 5 that differential thermistors were used for this heat pipe. The measured ΔT's of 1.5 to 2.5° C between various parts of the structure tube verified that the heat pipe was working as expected in flight.

Table 5

Level 4 Heat Pipe Testing – Flight and Ground Results.

Power (Watts)	Channel/ΔT Locations	Flight - ΔT* ° C (absolute values)	FTV - ΔT† ° C
18	1: STR/PIPE att E BAY	1.9	1.5
	2: Pipe/Pipe E to D/E	3.2	3.5
	3: Pipe/Pipe D/E to D	0.8	1.0
	4: Pipe/STR at D BAY	0.8	0.9
	5: Structures A to E.	0.8	1.6
36	1	2.4	1.8
	2	3.3	3.3
	3	1.0	0.8
	4	0.6	0.4
	5	0.9	1.3
55	1	2.6	2.7
	2	5.1	5.1
	3	3.4	3.1
	4	0.1	0.2
	5	1.1	0.6
27	1	1.9‡	1.7
	2	3.8‡	4.3
	3	1.7‡	1.9
	4	0.4‡	0.6
	5	1.0‡	1.0
54	1	2.3‡	2.7
	2	4.6‡	5.1
	3	2.8‡	3.1
	4	0.0‡	0.2
	5	0.7‡	0.6

* Data date – September 1972.
† Data date – April 1972.
‡ Data date – October 1972.

Table 6

Level 5 Heat Pipe Testing – Flight and Subsystem Results.

Power (Watts)	Flight ΔT ° C September 1972	Subsystem ΔT ° C February 1971
19	3.5	2.5
33	2.2	3.2
52	2.2	3.5
79	2.3	Dryout
	October 1972	February 1972
26	3.1	3.2
50	2.2	3.5
79	2.2	Dryout

Level 5 Heat Pipe Flight Data

Data from the level 5 heat pipe is given in Table 6. A cross-sectional view of this pipe is shown in Figure 5(a-1). Unfortunately, no comparable ground test data is available from the FTV test due to operational problems. In the FTV test, the heat pipe suffered a dryout at low power conditions and never functioned as expected after repriming was attempted. Many tests were also carried out on this pipe as a subsystem, and many of these tests resulted in failure of the pipe to perform properly. However, some useful flight heater test data were obtained, and where applicable, these data are presented in Table 6 for comparisons.

To date, the zero-G flight tests results are good. The circumferential temperature differences, ΔT's, were low, and the pipe carried more heat at lower ΔT's in orbit than in a 1-G environment.

Table 7

Level 6 Heat Pipe Testing - Flight and FTV Ground Results.

Power (Watts)	Flight ΔT ° C September 1972	FTV ΔT ° C April 1972
19	1.9	1.5
40	5.6	–
59	8.0	–
90	9.1	9.3
	October 1972	April 1972
34	4.6	–
26	1.7	1.5
59	6.6	–
90	9.1	9.3

Level 6 Heat Pipe Flight Data

Recorded flight data compares favorably with FTV data. A cross-sectional view of this pipe is shown in Figure 5(a-2). The ΔT's for this pipe with spacecraft heat loads only (~ 19 W) were approximately half the corresponding level 5 ΔT's. Power loads for this pipe were greater than those recorded for the level 5 pipe. Instrumentation of the level 5 and 6 pipes is very similar, so that data from these pipes should compare favorably. However, once the large F/G bay flight heater was energized, the level 6 ΔT was considerably higher than that recorded for the level 5 pipe; the level 6 ΔT was also higher during the FTV test. This result was considered to be an anomaly due to thermistor heating by conduction from the energized heater through the tape holding the heaters and thermistors in position. No physical correction to the tape was attempted before launch since possible heater damage was feared. (For further information on this phenomenon, see Reference 28).

Other than the anomalous level 6 ΔT, the pipes performed reasonably well in both 1-G and zero-G environments, and the data comparisons are good.

Test Results – Summary

Test results from the orbiting spacecraft have shown that the heat pipes used on OAO-C are functioning as expected and compare favorably with ground test results. The main problem associated with the orbital data is the lack of instrumentation. This problem does inhibit the data comparisons to a certain degree, but is basically overcome by carefully selecting the location of each thermistor. The performance of the three pipes can be summarized briefly as follows:

- Flight data and ground data results compare favorably
- Data analysis shows that the pipes are isothermalizing the structure tube
- No measurable degradation has been recorded

Goddard Space Flight Center
National Aeronautics and Space Administration
Greenbelt, Maryland November 20, 1972
831-41-25-02-51

REFERENCES

1. G. Yale Eastman, "The Heat Pipe," Scientific American, 218, 5, May 1968.

2. G. M. Grover, et al., "Structures of Very High Thermal Conductance," J. Appl. Phys., 35, 1964.

3. Feldman and Whiting, "The Heat Pipe," Mechanical Engineering, February 1967.

4. Feldman and Whiting, "Applications of the Heat Pipe," Mechanical Engineering, November 1968.

5. R. C. Turner, "The Constant Temperature Heat Pipe—A Unique Device for the Thermal Control of Spacecraft Components," AIAA 4th Thermophysics Conference, June 1969.

6. Norman H. Abramsom, "The Dynamic Behavior of Liquids in Moving Containers," NASA SP-106, 1966.

7. E. D. Waters, "Design, Fabrication, and Testing of ATS-E Solar Panel/Heat Pipe Substrates," Summary Report for NASA, DAC-63370, June 1969.

8. W. B. Hall, "Heat Pipe Experiments," Radio Corporation of America.

9. T. P. Cotter, "Theory of Heat Pipes," Los Alamos Publication LA-3246-MS, March 1965.

10. T. P. Cotter, "Heat Pipe Startup Dynamics," Thermionic Conversion Specialist Conference, Palo Alto, California, October 1967.

11. J. E. Kemme, "High Performance Heat Pipes," Thermionic Conversion Specialist Conference, October 1967.

12. S. Katzoff, "Heat Pipes and Vapor Chambers for Thermal Control of Spacecraft," AIAA Paper No. 67-310, April 20 1967.

13. S. Katzoff, "Notes on Heat Pipes and Vapor Chambers and Their Application To Thermal Control of Spacecraft," NASA, Langley Research Center Paper No. 67-26796.

14. J. E. Kemme, "Heat Pipe Capability Experiments," Los Alamos Publication LA-3585-MS, October 1966.

15. William H. McAdams, "Heat Transmission," Third Edition, New York, 1954.

16. J. L. Anderson and E. Lantz, "A Nuclear Thermionic Space Power Concept Using Rod Control and Heat Pipes," NASA TN D-5250, May 1969.

17. F. G. Arcella and G. S. Dzakowic, "Heat Pipe Function Isothermally and Adaptably," Research and Design Trend, August 1969.

18. J. E. Kemme, "Heat Pipe Design Considerations," Los Alamos Publication LA-4221-MS, August 1, 1969.

19. D. K. Anand, "On the Performance of a Heat Pipe," Engineering Notes, December 1965.

20. Max Jakob, "Heat Transfer," New York, 1949. Vols. I, II.

21. T. P. Cotter, "Heat Pipe Startup Dynamics," Thermionic Conversion Specialist Conference, October 1967.

22. Sir Horace Lamb, Hydrodynamics, New York, 1932.

23. E. E. Gerrels and J. W. Larson, "Brayton Cycle Vapor Chamber (Heat Pipe) Radiator Study," NASA CR-1677, February 1971.

24. J. P. Marshburn, "Results of Thermal Vacuum Testing the OAO-C Dynatherm Heat Pipe," NASA/GSFC Memorandum, February 1971.

25. J. P. Marshburn, "Results of Thermal Vacuum Testing of the Grumman OAO-C Structural Heat Pipe," NASA/GSFC Memorandum, November 1971.

26. J. P. Marshburn, "Test of the Redesigned Level-6 Grumman Spiral-Artery Heat Pipe Under Thermal Vacuum Conditions," NASA/GSFC Memorandum, December 1971.

27. Goddard Space Flight Center, Specification OB-A-0086-C, OAO-C Heat Pipe, September 18, 1970.

28. 30 DAY REPORT OAO-3, Vol II., Grumman Aerospace Corp. for Goddard Space Flight Center under Contract NAS5-814.